Tile Hamiltonian for Decagonal AlCoCu

Ibrahim Al-Lehyani[a,b] and Mike Widom[a]

[a]*Department of Physics, Carnegie Mellon University, Pittsburgh, Pennsylvania 15213*

[b]*Department of Physics, King AbdulAziz University, Jeddah, Saudi Arabia*

(March 13, 2002)

Abstract

A tile Hamiltonian (TH) replaces the actual atomic interactions in a quasicrystal with effective interactions between and within tiles. We studied AlCoCu decagonal quasicrystals described as decorated Hexagon-Boat-Star (HBS) tiles using ab-initio methods. The dominant term in the TH counts the number of H, B and S tiles. Phason flips that replace an HS pair with a BB pair lower the energy. In Penrose tilings, quasiperiodicity is forced by arrow matching rules on rhombus edges. The edge orientation in AlCoCu is due to Co/Cu chemical ordering. Tile edges meet in vertices with 72° or 144° angles. We find strong interactions between edge orientations at 72° vertices that force a subset of the Penrose matching rules. Interactions at 144° vertices are somewhat weaker. The "vertical" edge orientation disorder interactions are intermediate in strength.

I. INTRODUCTION

Both quasicrystals and ordinary crystals are made of elementary building blocks. In crystals, a single unit cell is arranged side by side to cover the space periodically. Two approaches to build quasilattices are proposed. One uses a single unit cell but allow adjacent cells to overlap. Gummlet [1] proved that using a limited number of overlapping positions between decagons produces a quasicrystal structure. Steinhardt and Joeng [2] further proved that the overlapping conditions can be relaxed and supplemented by the maximizations of a specific cluster to produce quasilattices. This is the "quasi-unit cell" approach and slightly different but conceptually similar is the covering approach.

In the tiling method the space is covered with a limited number of tiles. No overlapping is allowed and depending on the way the tiles are arranged quasicrystal structures can be produced. Matching rules between tiles govern the local tile configurations by allowing a subgroup of all possible ones. Globally, they enforce quasiperiodicity. Penrose proposed his famous matching rules before the discovery of quasicrystal materials. In 2D, Penrose tiles are a fat and a thin rhombi (Fig 1a). Edges are assigned arrow decorations and they must match for common edges in adjacent tiles. In perfect quasicrystals these rules are obeyed everywhere. However in the construction process one might have freedom of choice at one point that will affect future configurations. Thus backward tracking and correction procedures are needed when a conflict is reached because it might be a result of what appeared to be a degenerate choice in an early stage.

The very restrictive Penrose matching rules are sufficient but not necessary for quasiperiodicity. Socolar [3] showed that weaker matching rules can still produce quasilattices. The less restrictive set of rules are derived by allowing bound fluctuations in perp space.

The tiling description is based on entropical considerations. The energy assignment to matching rule violations must be realized physically. Burkov [4] proposed matching rule enforcement by chemical ordering of CoCu pairs in AlCoCu. However that model involved an unnatural symmetry linking Co sites to Cu sites. Cockayne and Widom [5] deduced a different, physically realistic, type of CoCu ordering. In their model, tile edges are assigned arrow direction based on their Co/Cu decorations (Fig.1b). The physical origin of Co/Cu chemical ordering rests on the status of Cu as a Noble Metal with completely filled d orbitals unlike normal transition metals such as Co.

In quasicrystals, the actual atomic interactions in system Hamiltonian can be replaced with effective interactions between and within tiles. The resulting tile Hamiltonian is a rearranged original Hamiltonian. In simple interaction pictures (pair potentials for example) the relation between the two is straight forward. It might be difficult for more complicated potential descriptions to find the relations between them but it is theoretically possible. The tile Hamiltonian includes terms which depends only on the number of tiles and other terms for different interactions. The tile Hamiltonian simplifies the picture greatly and it is a reasonable way to describe the tiles.

Space can be tiled in many different ways. Even when holding the number of atoms or the number of similar tiles fixed. Figure 2 shows three tiling configurations of 132 atoms. These are called quasicrystal approximants which are crystals that are very close to quasicrystals in properties. One of their advantages is that they can be studied using the same conventional tools. The first two have the same number of tiles are arranged differently.

In a previous paper [9] we studied the matching rules in decagonal AlCoCu using a limited group of quasicrystal approximants. Some angle interactions details couldn't be extracted. Here we study more thoroughly the set of rules controlling these compounds using different techniques and a much bigger set of approximants.

First, we describe the model of decagonal AlCoCu in section II. Section III gives our detailed calculations using ab-initio methods. Similar calculations but using pair potentials to compare with are described in section IV.In section V, we talk about different other effects to be considered in the model. We analyze our finding and study their implications on AlCoCu compounds in section VI

II. DECAGONAL AL-CO-CU

Decagonal Al-Co-Cu quasicrystals have been studied by many, theoretically [7] and experimentally [8]. Cockayne and Widom [5] proposed a model based on tiling of space by Hexagon, Boat and star tiles (HBS) decorated deterministically with atoms 2. The tile edge length is 6.4 Å.Tile vertices are occupied by 11-atom clusters. Each cluster consists of two pentagons of atoms staked on each other and rotated by 36°. One layer contains only Al atoms and the other layer contains a mixture of TM and can contain Al atoms. The mixed Al/TM decagon contains an additional Al atom at its center. Decagons meet with pairs of Co-Cu at about 2.6 Å apart. Tile edges are drown by these pairs and they are 6.4 Å long in quasiperiodic plane and $\frac{1}{2}c$=2.08 Å along the periodic direction. All TM atoms surrounding a vertices Al atom are parts of tile edges. It was shown in the original model that TM atoms prefer to alternate on tile edges. This was confirmed later using locally self-consistent multiple scattering (LSMS) method [9] and again in this study.

We assign arrows to edges based on the TM atom decorations. By our definition, an arrow points from Cu to Co atoms. Tile edges meet in vertices at 72° or 144° angles. An angle is of type "i" if both edges point in towards their meeting vertices. Types "o" and "m" are out and mixed pointing.

Hexagon, boat and star tiles are the building blocks in the model. The HBS tiles are composed of Penrose tiles with double arrows satisfied (by definition) inside the tiles. Some of their properties are summarized in table I. The space can be constructed then by only watching out for the single arrows (Fig. 1).

We choose to define a tile Hamiltonian for the system

$$H = \sum_{\alpha} n_t^{\alpha} E_t^{\alpha} + \lambda_1 \sum_{\beta} n_{72}^{\beta} E_{72}^{\beta} + \lambda_2 \sum_{\beta} n_{144}^{\beta} E_{144}^{\beta}. \tag{1}$$

Here n_t^{α} is the number of specific tile type α which can be s, b or h; n_{72}^{β} and n_{144}^{β} are the numbers of 72° and 144° angles and β is the angle orientation. We fit the Hamiltonian 1 to achieve $H \approx E_{tot}$. The tile energies are much bigger than the other terms and it turns out that the 72° angle interactions are bigger than the 144°'s. It is desirable to check how every term can alter the system energies. We set λ_1 and λ_2 to 1 or 0 for the purpose of including and excluding the angle interactions.

A hexagon contains 25 atoms, counting those on the perimeter fractionally. All but 3 atoms (one Al and 2 Co) belong to vertex decagons. The Co atoms occupy symmetric sites and the Al atom breaks the symmetry by residing on one of two geometrically equivalent positions between the two Co atoms(1b,left). Its interaction with tile edge TM atoms determines the preferred position. A boat has 41 atoms. An internal Al atom breaks the symmetry(1b, center) by residing in one of two equivalent sites. A star has 57 atoms. In a star, two internal Al atoms break the symmetry(1b, right) by occupying any two of five equivalent sites as long they are 144° apart.

A phason flip can switch a specially arranged star and a hexagon to a pair of boats. This is shown in fig 2 outlined by a dashed line. The presented structure is slightly different form the original model. There Cu atoms takes symmetry breaking positions inside the boat and the star. Composition is not conserved under a phason flip between boats and stars. As discussed above, in our model Cu atoms reside only on tile edges and symmetry is broken by the internal Al atoms.

Many different quasicrystal approximants are exploited here to study different terms in tile Hamiltonian. All the approximants are listed in table II with some of their properties. The choice is based on the information which can be extracted from any approximant. The smallest structure is the monoclinic single-hexagon approximant (Fig.3). It contains one horizontal and two inclined tile edges. For the decoration shown, equation (1) becomes

$$H = E_t^h + \lambda_1(E_{72}^i + E_{72}^o) + \lambda_2(2E_{144}^i + 2E_{144}^o) \tag{2}$$

The next bigger approximant is a 41-atom single-boat (Fig 4). Single stars do not cover the space so a single-star unit cell approximant is not possible. Two-hexagon approximants can be constructed in orthorhombic cells either by a genuine orthorhombic structure (Fig 5) or by doubling a monoclinic cell (Fig 3). The doubling process gives more freedom in controlling edge arrow orientations by performing Co/Cu swaps. Similarly a two-boat unit cell can be constructed either by doubling the single boat structure or by tiling the two boats like in b2 (Fig 6).

To isolate the angle interaction parameters, larger approximants are needed. The three approximants in fig 2 have 132 atoms per unit cell but different tile configurations. Two of them are related to each other by a single phason flip (s1h3 and b2h2-2). The phason flip lowers the energy which indicates that stars are disfavored in these compounds. Angle orientations are investigated by swapping a TM pair on tile edges. Arrows in turns flip directions.

Long range interaction and other smaller terms in the tile Hamiltonian are estimated from swapping pairs surrounded by symmetric bonds on their sides. The bonds on the sides of the horizontal tile edge of h2 can be specially arranged to cancel the 144° interactions and leave only other effects.

III. AB-INITIO STUDY

For our calculations we employ ab-initio pseudopotential calculations utilizing the Vienna Ab-initio Simulation Package (VASP) program [10]. We use ultra soft Vanderbilt type pseudopotentials [11] as supplied by G. Kresse and J. Hafner [12]. Our calculations are carried out on the T3E and on the newly installed TCS machines at the Pittsburgh Supercomputer Center. The k-space mesh size (among other parameters) determines the accuracy of the calculations. Bigger k-space grids are more accurate but more expensive in calculation times. One has to balance between the number of atoms in a unit cell and the size of the k-space grid to fit within the available computer resources. As explained before, we use many different approximants for our study. The k-space mesh is increased until a consistency of about 0.02 eV is reached in worst cases. But within a reasonable use of our allocated times we are able to get better convergence (0.002-0.01 eV) for most structures.

The convergence pilot calculations are outlined in table III for our b1 structures and in table IV for our b2h2-1. There are two slightly different structures per approximant. They differ by a single arrow decoration (circled in Fig. 6 and Fig. 2a). The tables show that at the the chosen k-space grid used in our calculations (marked by a star in the tables), the accuracy is better than 0.02 eV. The smallest grid of 1x1x1 (single k-point in the middle of the k-space unit cell) for our b1 approximant takes about 8 minutes on the T3E machine (450 MHz alpha processors) using 8 processors. The largest grid we use for b1 of 5x5x15 (188 independent k-point) takes 4.8 hours on 64 processors. The b2h2-1 has 132 atoms per unit cell. The largest grid of 2x2x10 (20 independent k-points) takes about 6 hours on 64 processors. The smallest 1x1x1 grid takes 2 hours on 8 processors.

We note that for the same number of processors calculation time scales linearly with the number of independent k-points. But for the same structure calculation time decreases linearly (almost) with increasing number of processors only up to 16 processors. Beyond that, the total charging time (no. of processors*elapsed time) increases notably. Large structures and big k-space grids must use large numbers of processors because they need more memory. Another thing can be noted from tables III and IV is that the smoother the distribution of the k-space grid points along kx,kx and kz the closer the result to convergence. For our b1 approximant, meshes isotropically distribute k-space points are 1x1x3 and its multiples. For fixed number of kx and ky points the numbers get closer to converging results as we move kz to its isotropic value. In all our structures we choose the most homogeneous distribution of k-space points possible.

Many different rearrangements of arrows, by swapping TM atom pairs, are performed and the different structure energies are calculated. Most of these are done for the large approximants because they give more freedom. In general, pure 72° angle interactions can be deduced if the middle bond has an equal number of 144° connections on each side (since we can arrange for 144° interaction to cancel) and either a total of one 72° connection which can be attached to any side or two from the same side. An example is outlined by a dashed rectangle in Fig. 2a. The bond is surrounded by a single 144° on each side. Both point towards the middle bond making i144 on one side and m144 on the other. One extra 72° on one side makes o72. If the middle pair is swapped the 144° angle interactions will be conserved. The swap merely switches their sides. The o72 becomes m72. The difference between the swapped and the basic structures is the difference between m72 and o72. Arranging the 72° outer bond further and then making the swap can give m72-i72. We can also arrange bonds to give an independent pure i72-o72 difference. For pure 144° interactions we use a middle bond surrounded by two 144° on one side and a single 144° connections from the other side. We arrange for any 72° angles to cancel. The pair surrounded by a dashed circle in Fig. 2a is one example that yields o144-m144.

We compute an over complete set of structures and use a least square fit. First, we fit with λ_1 and λ_2 in equation (1) set to zero, leaving only three adjustable parameters E_t^h,E_t^b and E_t^s. The fit is to find the best value of out parameters that minimizes the root mean square of the difference between the calculated E_{tot} and the model H. The fitting is shown in Fig. 7. The five figures correspond to the different energy ranges our approximants span. The large approximants spread over a large range of energies because of the freedom we have in different swaps. That's why the range of the first graph is six times bigger than the range of the rest. The first graph shows that a pair of boats is favored over a star and a hexagon. Both have the same number of atoms but the last has one more 72° interaction. The graphs also show clearly that the three-parameter fit is not adequate. Note that the values of h, b and s are individually meaningless. For example, the data quoted does not include arbitrary offsets EATOM of each chemical species. However, the difference 2b-h-s is meaningful.

The next set of graphs in Fig. 8 shows the fitting when we set λ_1 and λ_2 to one. The graphs are on different scales and the deviation from the y=x line is due to other longer-range effects. The root mean square of the deviations is 1.3×10^{-3}. In the first graph in Fig. 8 we intentionally control the swaps for all approximants to spread over the whole range. Such spread is not always possible depending on structure symmetry.

The different parameters are listed in table VI. The different energy constitutes of the model are as expected, tile energies are the biggest contribution. That is the first term in equation(1). The 72° angle orientation comes next. Then by an order of magnitude from it follows the 144° angle contributions. The inward configurations are highly disfavored and outwards are lowest in energy by the same magnitude. Mixed arrowing are almost zero in energy. In a previous paper [13], Co-Cu interaction was assumed to be the average of Co-Co and Cu-Cu interactions. This shows that such an assumption is very close to reality.

IV. PAIR POTENTIALS

The electronic ground state of a system can be expanded in terms of a volume energy and potentials describing n-body (n=2,3,4,...) interactions [14]. The volume energy accounts for the bulk part of the total energy. It depends on the density but bot the structure. Th n-body interactions distinguish between the different crystal structures at the same density. It is customary to truncate this at the pair potentials. the custom arose from the fact that they are much easier to calculate and use and higher order interactions are weak. Even for transition metals with the localized d-band, the decomposition to pair potentials proved to be practical [6]and [15].

Many different pair potentials have been used to study this and other quasicrystals. Cockayne and Widom [5] used mock-ternary potentials extracted from AlCo pair potentials. In Al-Co-Cu, Cu substitutes for an equal combination of Al and Co. So they approximated Cu interactions by the average interactions of Al and Co. They adopted AlCo pair potentials calculated by Phillips and others [16]. Alternation of TM atoms on tile edges and the effect of edge decorations on the central Al are all consistent with our VASP results.

Later, more rigorous pair potentials in the context of Generalized Pseudopotential Theory (GPT) were used for Al-Co-Ni [6]. The original GPT pair potentials suffered from TM overbinding which is an unphysical attraction between TM atoms at small separations. The strongest overbinding appears in Co-Co pair potentials. We modified the TM pair potentials at short distances by adding a repulsive term using VASP to get the energy and length scale [6]. Resulting potentials behave really well in the simulation [17].

We calculated the energies of the approximants using both mock-Ternary and modified

GPT pair potentials to check how the pair potentials will do compared to VASP. Structures are calculated at fixed volume and composition which enables us to ignore the volume term. Using the modified GPT, TM atoms favor alternation on the tile edges by 0.022 eV/cell for mGPT and 0.079 eV/cell for mock-Ternary. The central position for the Al atom is preferred by at least 0.11 eV/cell and 0.01 eV/cell..

Graphs in figures 10 and 9 show result fitting. Pair potentials give very good agreements between the model and the calculations even for the mock-ternary pair potentials.

Results of the fitting are summarized in table VI for all the methods used. Aside from a constant factor between the modified GPT and the mock-ternary pair potential calculations, they are very close to each other. The order of $144°$ angle interaction is reversed compared to VASP but these interactions are very weak

V. OTHER EFFECTS

In our model the source of matching rules is the chemical ordering of TM atoms on tile edges. We study chemical ordering here using our h2-1 approximant (The orthorhombic unit cell in fig 3). In Fig. 3, the heavily dashed unit cell is our h2-1 approximant. It contains two horizontal tile edges. A Cu atom from one of them is swapped with the Co atom on the other. Resulting edges contain pairs of similar species. The process raises the energy by 0.681 eV/cell. The same swap were studied before with LSMS [9] and gave same conclusion with different value (0.168 eV/cell). In AlCoNi, pairs of Ni are slightly preferred over pair of CoNi pairs. As a result AlCoNi has no arrow decorations at low temperatures. Cu and Ni are adjacent in the periodic table but they are more notably different in their properties. In an isolated Ni atom, the 3d shell has six electrons and the 4s shell is filled. The partial filling of the d-band makes it contribute in interactions. The 3d shell in Cu is filled with electrons and the 4s has one electron which makes Cu act more like a simple metal. The d-band in buried and doesn't participate in interactions very much.

Another important issue is the position of the central Al atom inside a hexagon. We briefly touched it in section II. There are two symmetric positions between the two internal Co atoms, the Al atom takes one of these positions. If the horizontal edges are parallel the Al atom prefers to reside in the side where Co atoms are by about 0.03 eV. In the smaller tiling representation (τ^2 deflated [17], the TM pairs on edges becomes inside the smaller hexagons and the area inside the hexagons are decomposed into a boat and a star. The position of the internal Al atom specifies the decompositions and its hopping from one site to the other cause a phason flip between the small star and the small boat. The decomposition is lost by placing the Al atom exactly at the center of the hexagon but it is the lowest energy configuration. It lowers the energy by at least 0.2 eV. With the Al atom in the central position the effect of tile edge arrowing on it is minimal.

Another decomposition is decomposing the HBS tiles to Penrose tiling like in Fig. 1. Decomposing the Star and the boat is no problem. But the hexagon can be decomposed in two ways. We define the decomposition such that the central Al to be away from the internal Penrose vertices.

The position of the internal Al atom inside a hexagon together with the horizontal tile edge arrows draw a general direction for the hexagon. We noticed that generally hexagons like to align in our h2-1 structure. The effect is very small ($\approx$ 0.01 eV) but enough to account for some of the discrepancies in the calculations.

One more small effect appears in some of the 144° angle where two 72° angles shares one edge making one 144°. It is enforced to be out by its stronger constitutes. We have several of these in our 132 atom approximants. The shared edge affects the angle orientation of the outer edges. We calculate the difference o144-m144 with the shared edge pointing inward and outward. With outward pointing, o144-m144 equals -0.075 eV/cell. An inward middle edge raises the difference by 0.015 eV.

Up to now we only talked about the faults in the quasiperiodic plane. Pairs of TM atoms on tile edges are 1.51 Å apart on the quasiperiodic plane and 2.07 Å along the periodic direction. The lines connecting them make angels of 54° from the plane and a zigzag along the periodic axes. The vertices of the zigzag are alternating TM atoms. We turn our attention to atomic orders in this direction now. Approximant b2h2-1 (Fig. 2a) has a glide plane parallel to the long side of its unit cell that can be exploited for the purpose. We make one pair swap (call this pair pair a) and call the structure structure (A). Another structure (B) is made from b2h2-1 by swapping the glide-equivalent image of pair a (call it pair b). These two structures have equal energies by symmetry. Further, we build a 264 atom unit cell by stacking two 132 atom unit cells. it is built once by stacking an A layer over an A layer and another time by stacking a B layer over an A layer. In AA the vertical zigzag is conserved. In AB the zigzag sequence is violated twice, once along pair a and another time along pair b. The AA and AB structures are calculated with a k-point mesh of 2x2x5. The difference $E_{AB} - E_{AA}$ equals 0.392 eV/264-atom cell. A single violation costs 0.196 eV per 8 Åslap.

VI. DISCUSSION

We discuss here the implications of our findings on the structure of decagonal AlCoCu. The main result is that now energy can be calculated quickly and accurately for these compounds by adding the relevant terms using table VI.

Adjacent 72° angles either share the same vertices or point in opposite directions. The first is the hidden 144 ° we discussed above and the second form a zigzag of 72° angle. This can be seen in h2-1 structure where an infinite zigzag forms perpendicular to the hexagons. Due to the fact that m72 is very close to the average of o72 and i72, the middle edge decoration an isolated zigzag with any direction is degenerate. Similar argument apply to the case of 144° zigzag but the effect is much smaller.

The last point leads us to a bigger question about the importance of the 144° angle interactions. Most of the times bonds participate in combinations of 144° and 72° angles. The stronger interactions determine bond arrowing. When a bond is surrounded by a total of four 144° angles and no 72° the middle bond is a part of 144° zigzag and its decoration doesn't matter. An example of this is circled in Fig. 6. There is only one configuration where decorations is determined by 144° interactions which is the one we used to get pure 144° angle effects. These configurations are not very uncommon and as we showed including them in the fitting did improve it slightly.

However, at high temperatures the situation is different. Quasicrystals are believed to be stabilized by entropical contributions at high temperatures. Transition from crystal to quasicrystal phases are reported at about 1000K (ref). That correspond to about 0.1 eV. At such temperatures the 144° angle interactions are irrelevant because it is smaller that the energy fluctuations and the structure is determined primarily by its 72° angle interactions

Our model expectations are in agreement with calculated energies. Figure 8 shows that fore most of the structures the model energies fall near the y=x line. The worst deviation is about 0.1 eV. Out of that we account for 0.03-0.05 eV from the internal Al atom effects on tile edges. The rest can be a collection of long range interactions. We do see these collection of effects in many different instances. When calculating pure 72° angle interactions using the bond surrounded by a rectangle in Fig. 2a in two different approximants (b2h2-1 and s1h3). The environments are identical up to about 7 Å but a difference of about 0.02 eV between the two cases shows up.

Pair potential calculations show that they are capable of catching the dominant 72° interactions we are investigating with a lot less calculation times.

In our previous paper [9], we reported several results. Approximants h2-1 and h2-2 were used with internal Al atoms centered. The swap for chemical ordering agrees in sign but VASP's is four times bigger that LSMS. Other swaps give 2m72-i72-o72 agree in sign with the same factor disagreement in magnitudes.

Further studies might include the effect of TMAl arrows on tile edges. The difficulty in comes from the fact that such arrowing exist not only on tile edges but also inside the tiles.

ACKNOWLEDGMENTS

IA wishes to thank King Abdul Aziz University (Saudi Arabia) for supporting his study and MW acknowledges support by the National Science Foundation under grant DMR-0111198. We thank the Pittsburgh Supercomputer Center for the computer times for this study.

REFERENCES

[1] P.Gummlet, Geometria Dedicata **62**, 1 (1996) and P.Gummelt, Material Science and Engineering **294-296**, 250 (2000)

[2] P. J. Steinhardt and H.-C Joeng, Nature (London) 382, 431 (1996) and H.-C Joeng and P. J. Steinhardt, Phys. Rev. B **55**, 3520 (1999)

[3] E. S. Socolar, Commun. Math. Phys. **129**, 599 (1990)

[4] S.E. Burkove, Phys. Rev. B **47**, 12325 (1993)

[5] E. Cockayne and M. Widom, Phys. Rev. Lett. **81**, 598 (1998)

[6] I. Al-Lehyani, M. Widom, Y. Wang, N. Moghadam, G. M. Stocks and J. A. Moriarty, Phys Rev. B**64**, 075109 (2001)

[7] See for example: S. E.Burkov,Phys. Rev. B **67**, 614 (1991) and G. Zeger and H. -R. Trebin, Phys. Rev. B **54**, R720 (1996)

[8] See for example: K. H. Kuo and Z. Zang, Progress in Crystal Growth and Characterization of Materials, **34**, 191 (1997), H. Chen, S. E. Burkov, Y. He, S.J. Poon and G.J. Shiflet, Phys. Rev. Lett. **65**, 72 (1990) and K. Saitoh, K. Tsuda, M. Tanaka, A.P. Tsai, A. Inoue and T. Masumoto. Phil. Mag. A **73**, 387 (1996)

[9] M. Widom, I. Al-Lehyani, Y. Wang and E. Cockayne, Matter. Sci. Eng. A**295**, 8 (2000)

[10] G. Kresse and J. Hafner, Phys. Rev. B **47**, RC558 (1993); G. Kresse, Thesis, Technische Universität Wien 1993. G. Kresse and J. Furthmüller, Comput. Mat. Sci.**6**, 15-50 (1996). G. Kresse and J. Furthmüller, Phys. Rev. B **54**, 11169 (1996).

[11] D. Vanderbilt, Phys. Rev. B **41**, 7892 (1990).

[12] G. Kresse and J. Hafner, J. Phys.: Condens. Matter **6**, 8245 (1994).

[13] M. Widom, I. Al-Lehyani and J. A. Moriarty, Phys Rev. B**62**, 3648 (2000)

[14] J. Hafner, *From Hamiltonians to Phase Diagrams* (Springer-Verlag, Berlin Heidelberg, 1987).

[15] A. H. MacDopnald and Roger Taylor, Can. J. Phys. **62**, 796 (1984)

[16] R. Phillips, J. Zou, A. E. Carlsson, and M. Widom, Phys. Rev. B **49**, 9322 (1994)

[17] M. Mihalkovic,I. Al-Lehyani, E. Cockayne, C. L. Henley, N. Moghadam, J. A. Moriarty, Y. Wang and M. Widom, PRB to appear.

[18]

TABLES

TABLE I. Basic Tiles in HBS model and their compositions

tile	No. of Atoms	Composition	Penrose tiles
H	25	$Al_{17}Co_5Cu_3$	2T+F
B	41	$Al_{29}Co_8Cu_4$	T+3F
S	57	$Al_{41}Co_{11}Cu_5$	5F

TABLE II. The approximant tilings we use for our study and the number of different decorations (Nd) of each of them. The unit cells are either orthorhombic (a, b are given) or monoclinic (a,b and an angle are given). All of them have c=4.08 Å in the z-direction. The number of independent k-points is the number on which most of the structures are calculated. To investigate the convergence we go higher sometimes for couple structures (see tables IIIand IV).

Tiling	Nd	a, b (*theta*)	Composition	Indep. K-points	figure
h1	3	12.14, 7.50 (72°)	$Al_{17}Co_5Cu_3$	132	3
b1	6	12.13,12.13 (108°)	$Al_{29}Co_8Cu_4$	88	4
h2-1	5	23.08, 7.56	$Al_{34}Co_{10}Cu_6$	66	3
h2-2	4	14.27,12.13	$Al_{34}Co_{10}Cu_6$	66	5
b2	3	12.13,30.30 (134.5°)	$Al_{58}Co_{16}Cu_8$	55	6
b2h2-1	27	19.63,23.08	$Al_{92}Co_{26}Cu_{14}$	20	2a
b2h2-2	6	19.63,23.08	$Al_{92}Co_{26}Cu_{14}$	20	2b
s1h3	12	19.63,23.08	$Al_{92}Co_{26}Cu_{14}$	20	2c

TABLE III. Energies of approximant b1 and one of its variants (single swap). Our convergence pilot investigation goes through several k-point grids. Isotropic k-point distributions are 1x1x3 mesh and its multiples.

K-point grid	Indep. K-points	E_{b1}	$E_{b1-swapped}$	ΔE
1x1x1	1	-186.83238	-186.78158	0.05080
1x1x2	1	-217.02636	-216.68522	0.34114
1x1x3	2	-215.95009	-215.63608	0.31401
2x2x2	4	-218.18586	-217.90238	0.28348
2x2x4	8	-216.75311	-216.51774	0.23537
2x2x6	12	-216.74436	-216.49251	0.25185
3x3x3	14	-216.59210	-216.32712	0.26498
3x3x9	41	-216.74029	-216.48619	0.25410
4x4x4	32	-216.77625	-216.53784	0.23841
4x4x11*	88	-216.74116	-216.48698	0.25418
4x4x12	96	-216.74323	-216.48616	0.25707
5x5x15	188	-216.74291	-216.48615	0.25676

TABLE IV. Similar results for approximant b2h2-1.

K-point grid	Indep. K-points	E_{b2h2-1}	$E_{b2h2-1-swapped}$	ΔE
1x1x1	1	-606.30421	-606.22773	.07648
1x1x2	1	-704.05048	-703.77620	.27428
1x1x4	2	-700.48922	-700.24548	.24374
2x2x2	4	-704.02670	-703.77286	.25384
1x2x8	8	-700.38011	-700.12094	.25917
2x2x4	8	-700.73700	-700.49654	.24046
1x2x10	10	-700.42044	-700.15409	.26635
2x2x8	16	-700.44533	-700.18672	.25861
2x2x10*	20	-700.45159	-700.19033	.26126

TABLE V.

Parameters	3-para	6-para	9-para	10-para
h	-133.172	-133.150	-133.152	-133.151
b	-216.419	-216.760	-216.768	-216.768
s	-298.32	-300.082	-300.150	-300.152
2b-h-s	-1.34539	-0.288	-0.235	-0.233
i72	-	0.29428	0.294574	0.294691
m72	-	-0.034355	-0.0351678	-0.0352893
o72	-	-0.259925	-0.259406	-0.259402
i144	-	-	0.0371263	0.0368907
m144	-	-	-0.00277045	-0.00230114
o144	-	-	-0.0343558	-0.0345895
l-sym	-	-	-	-0.00286115
s.d.	0.36647	0.00261505	0.00132768	0.00132262

TABLE VI. The energy costs of different parameters in our model. All are 9-parameter fit

Parameters	Energy (VASP) (eV)	Energy (mGPT) (eV)	Energy (mock-T) (eV)
h	-133.152	-6.05162	2.12646
b	-216.768	-7.76726	5.23804
s	-300.150	-8.88991	8.48193
2b-h-s	-0.235	-0.59299	-0.13231
i72	0.294574	0.294217	0.0639178
m72	-0.0351678	0.00671985	-0.00707379
o72	-0.259406	-0.300937	-0.056844
i144	0.0371263	-0.0419126	-0.00793298
m144	-0.00277045	0.00952674	-0.0000801364
o144	-0.0343558	0.0323859	0.00801312

FIGURES

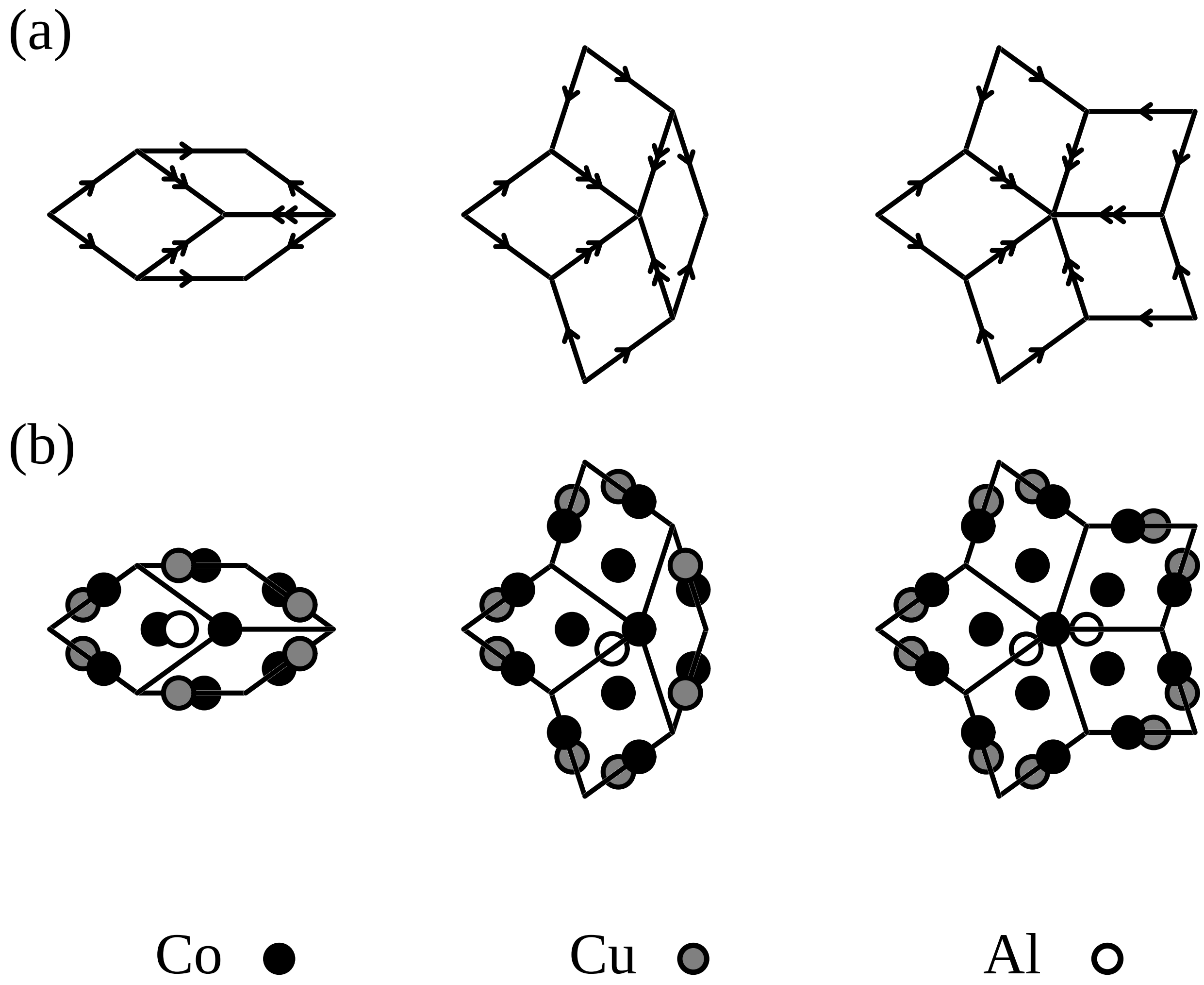

FIG. 1. HBS tiles and their decompositions to Penrose tiles (a) and atoms (b). In (b), only TM and Symmetry breaking Al atoms are shown.

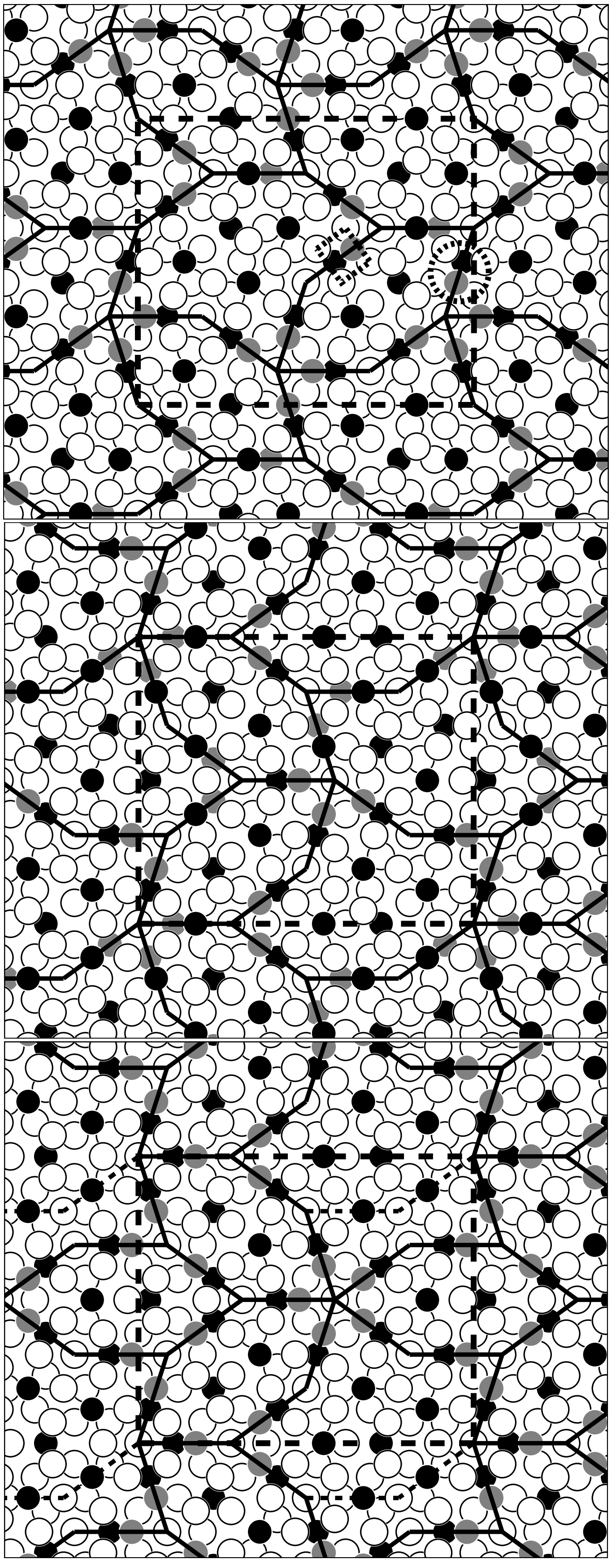

FIG. 2. Space can be tiled in many ways using HBS tiles. All these approximants (b2h2-1, b2h2-2 and h3s1) have 132 atoms per unit cell. Structures in (b) and (c) differ by a phason flip outlined in (c) with a small dashed line. Bonds in dashed shapes in (a) are bonds that can give information about pure angle interactions (after slight rearrangements)

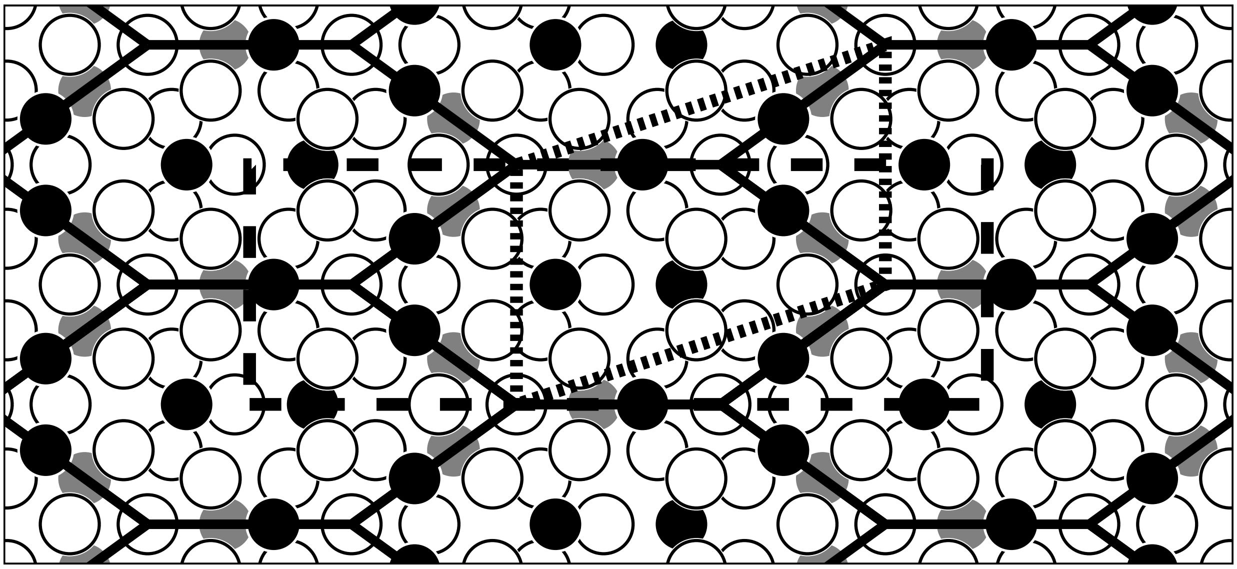

FIG. 3. Filling space with hexagons. This approximant has one hexagon per monoclinic cell (fine dashing, h1 structure in the text). The unit cell has 25 atoms. The cell can be doubled to get an ortho-rhombic unit cell (coarse dashing, h2-1 structure in the text).

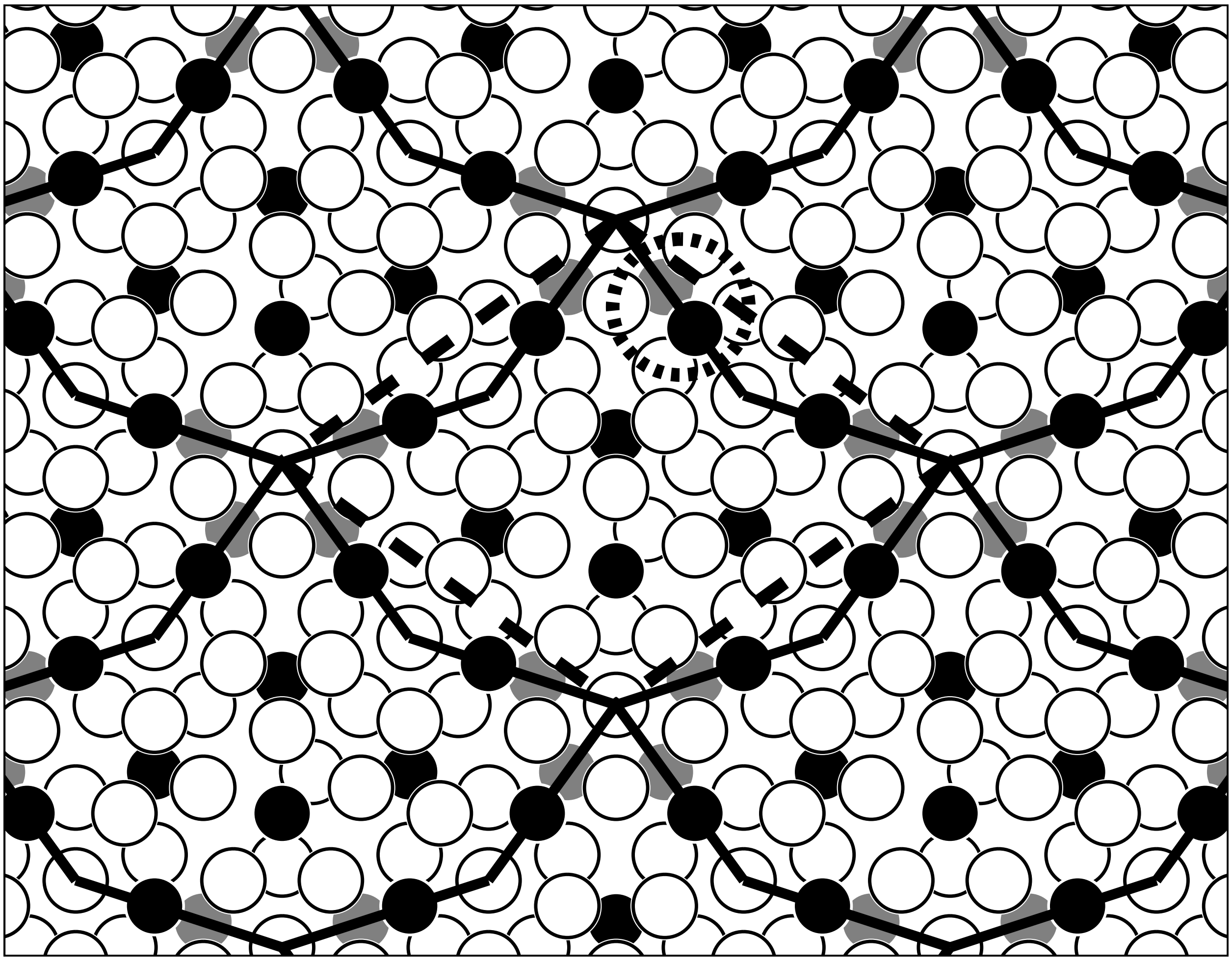

FIG. 4. Single boat (b1) approximant. It contains 41 atoms per monoclinic cell. Swapping the pair in the small rectangle changes the distribution of angle decorations. The two 144°'s surrounding the middle bond are images of each other. So total cancellation of 144° interactions is not possible in this unit cell. Enlarging the unit cell gives the freedom of assigning different decorations to the outer bonds to cancel that.

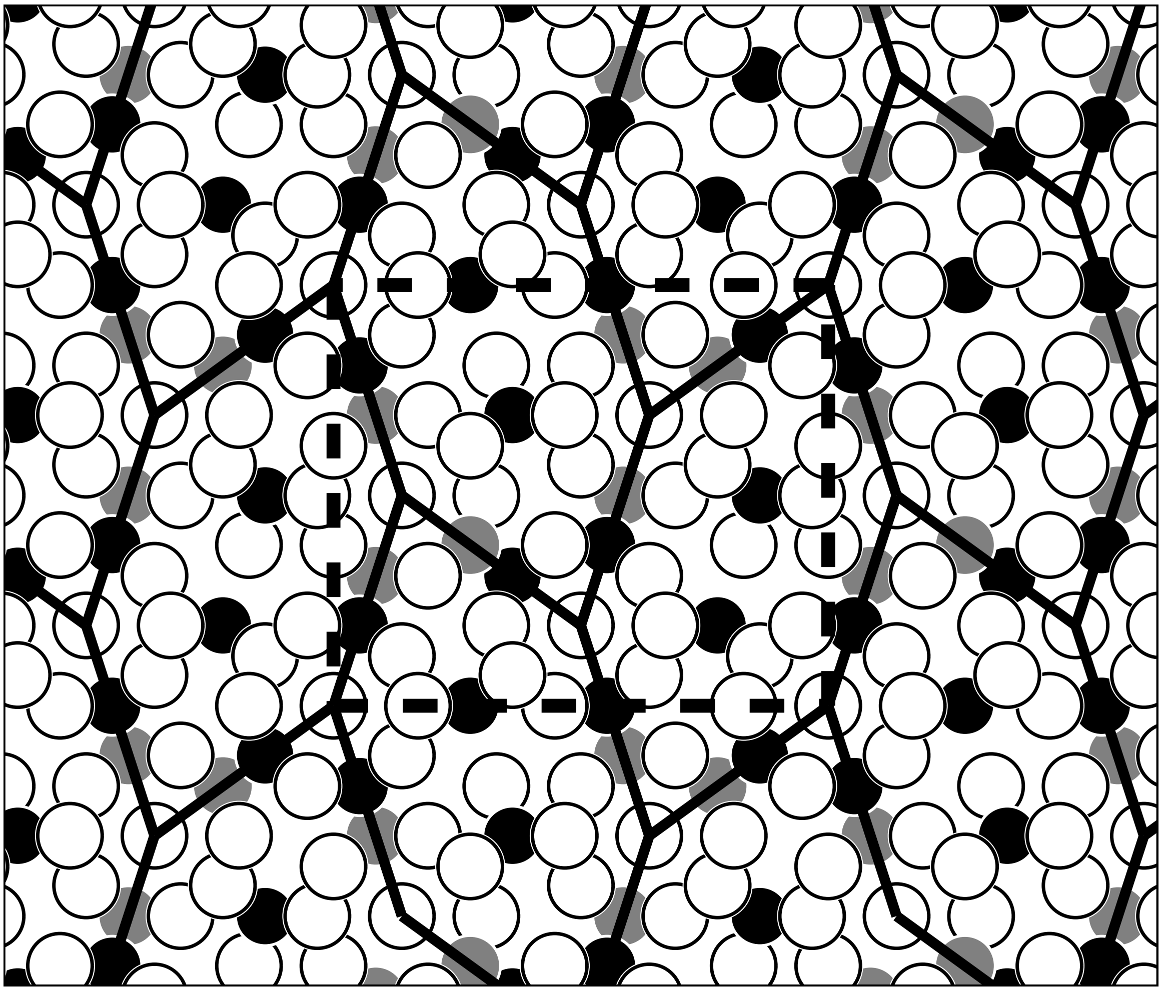

FIG. 5. Ortho-rhombic two hexagon approximants (h2-2). Different arrangements of hexagons from fig 3. Even with a single tile, space can be covered in different ways.

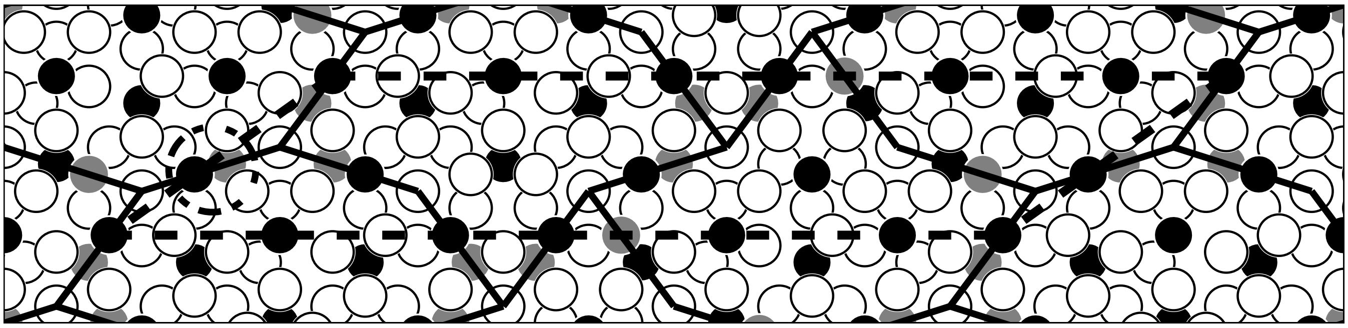

FIG. 6. Two boat approximant (b2). One of the heel bonds in the boats participates only in 144° angles.

Energies VASP

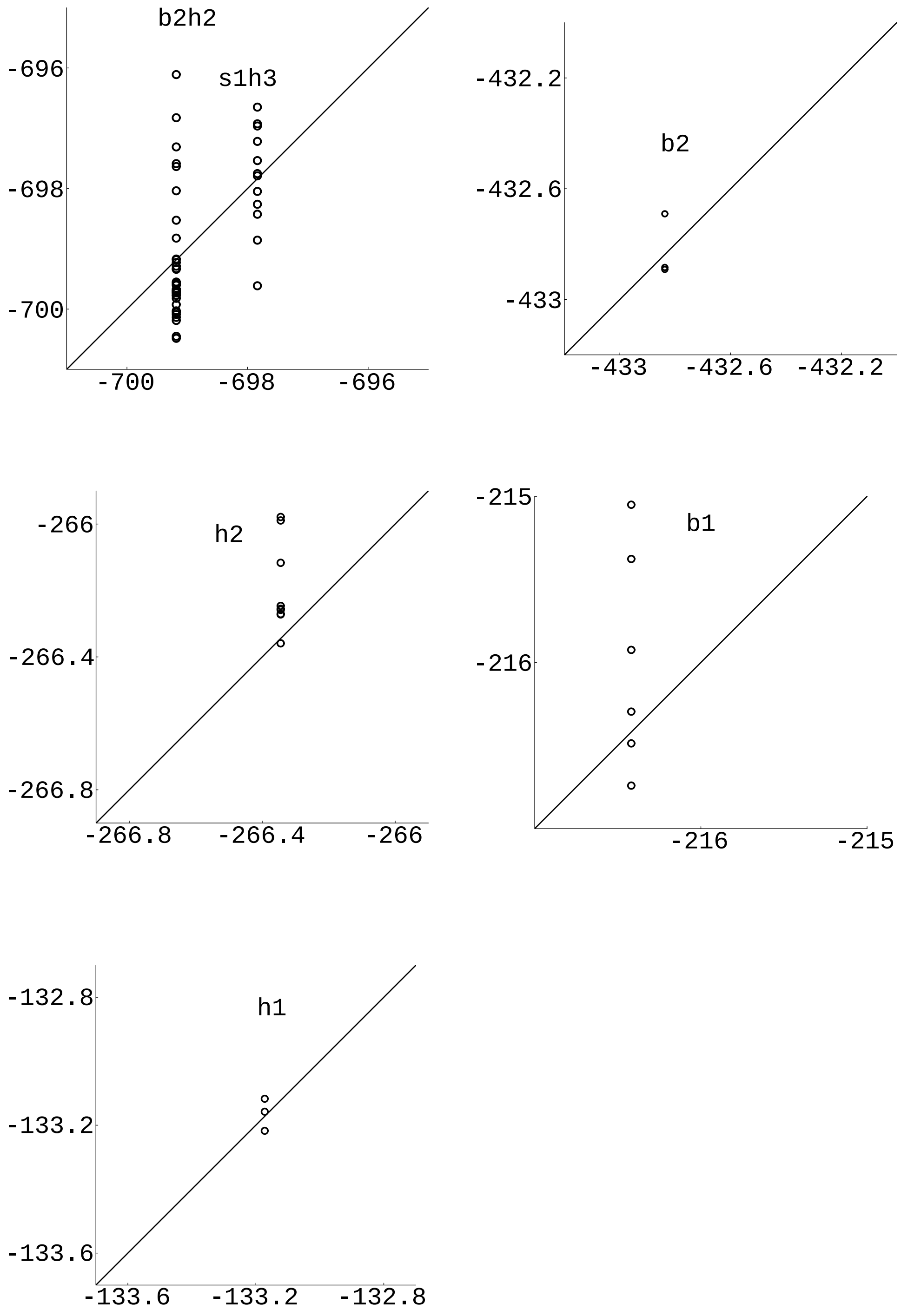

FIG. 7. plots of calculated structure energies vs. our model expectations using only tile energies (turning off angle interactions). The spread of energies vertically is due to angle contribution not accounted for in the model energies. The graphs in the set are on different scales to keep it consistent with the coming set of graphs.

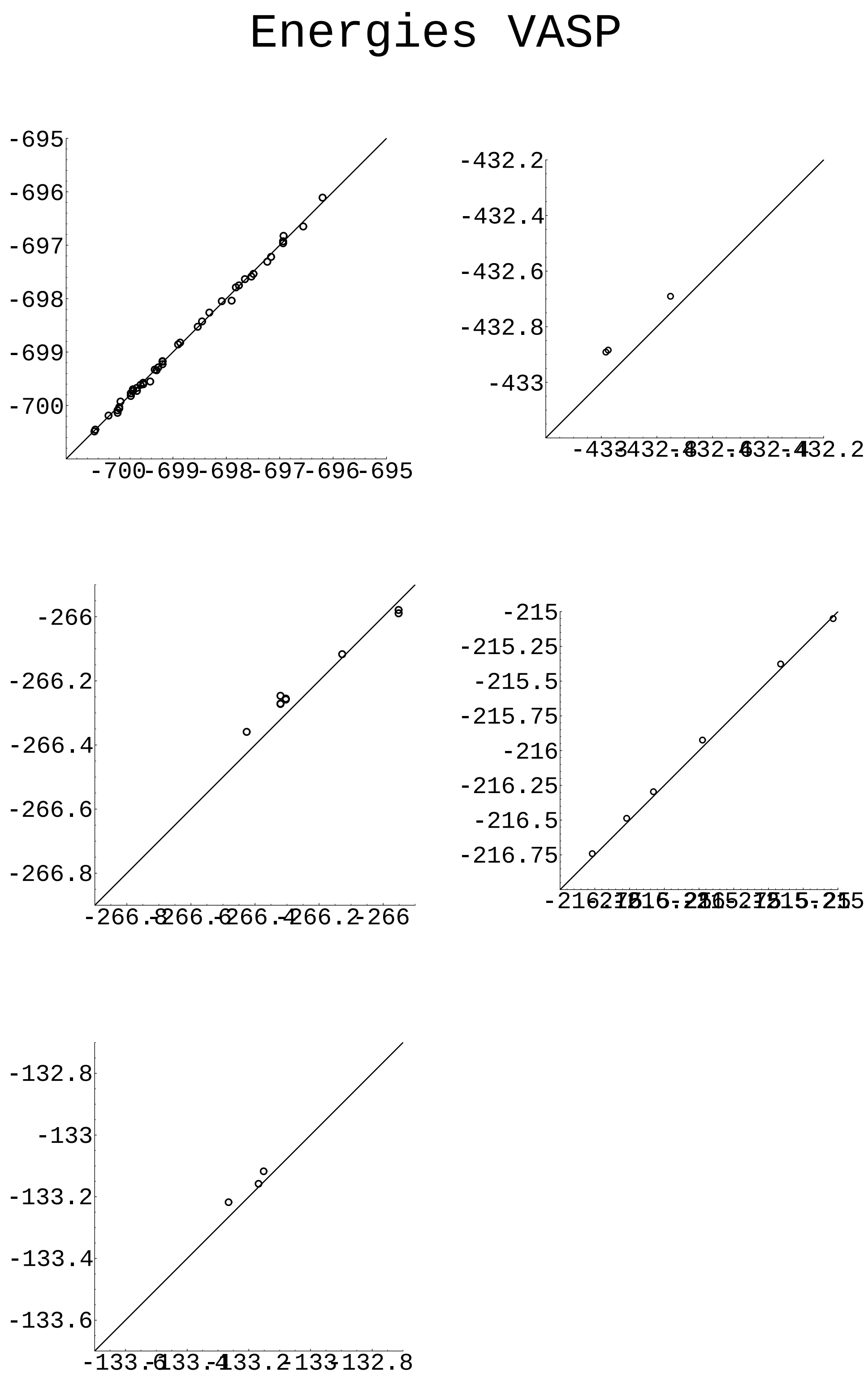

FIG. 8. Turning the angle interactions back on certainly improves the fitting. All the approximants in the first graph spread over the range shown for better comparison

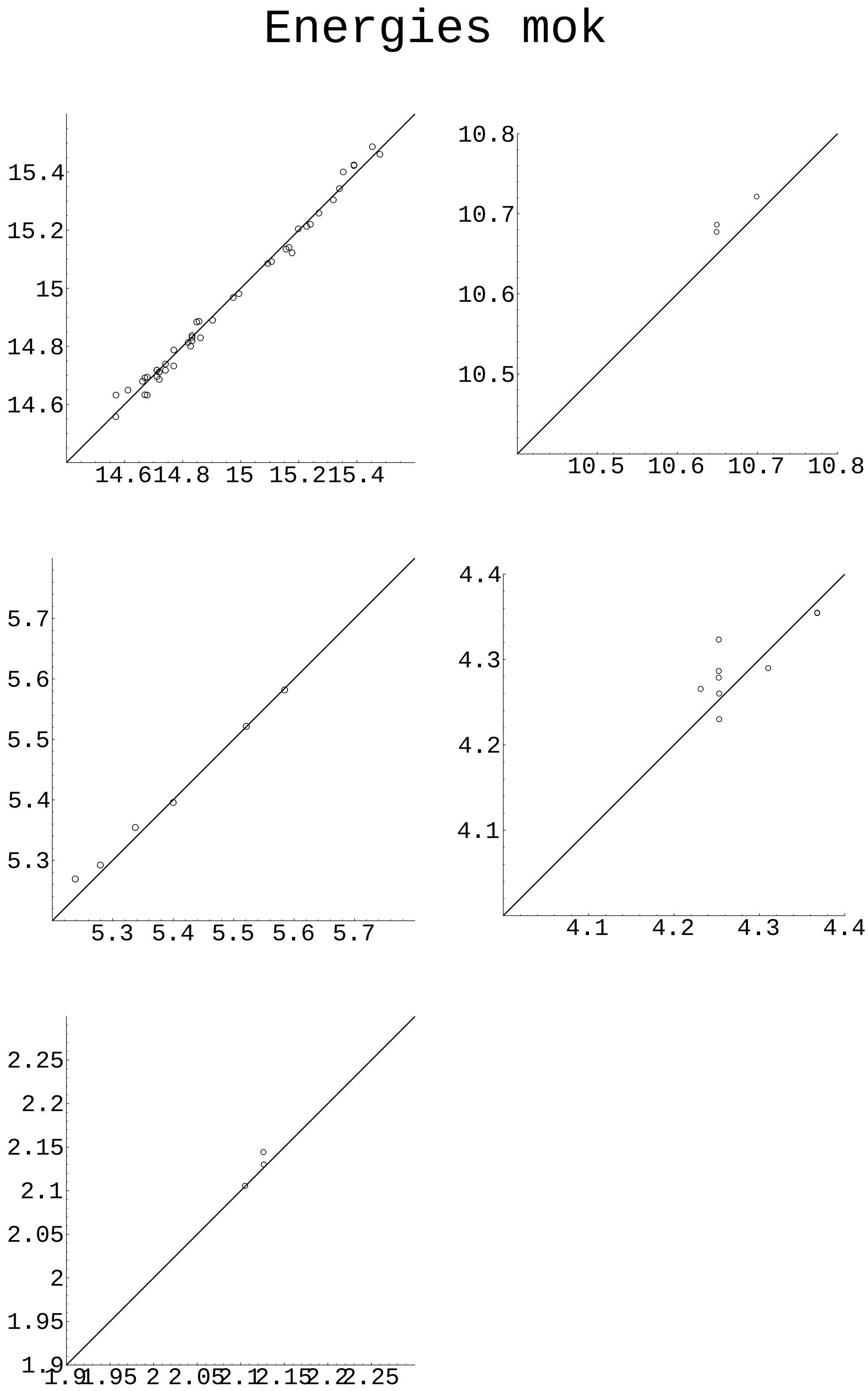

FIG. 9. Similar to figure 8 but for mock-ternary pair potential calculations

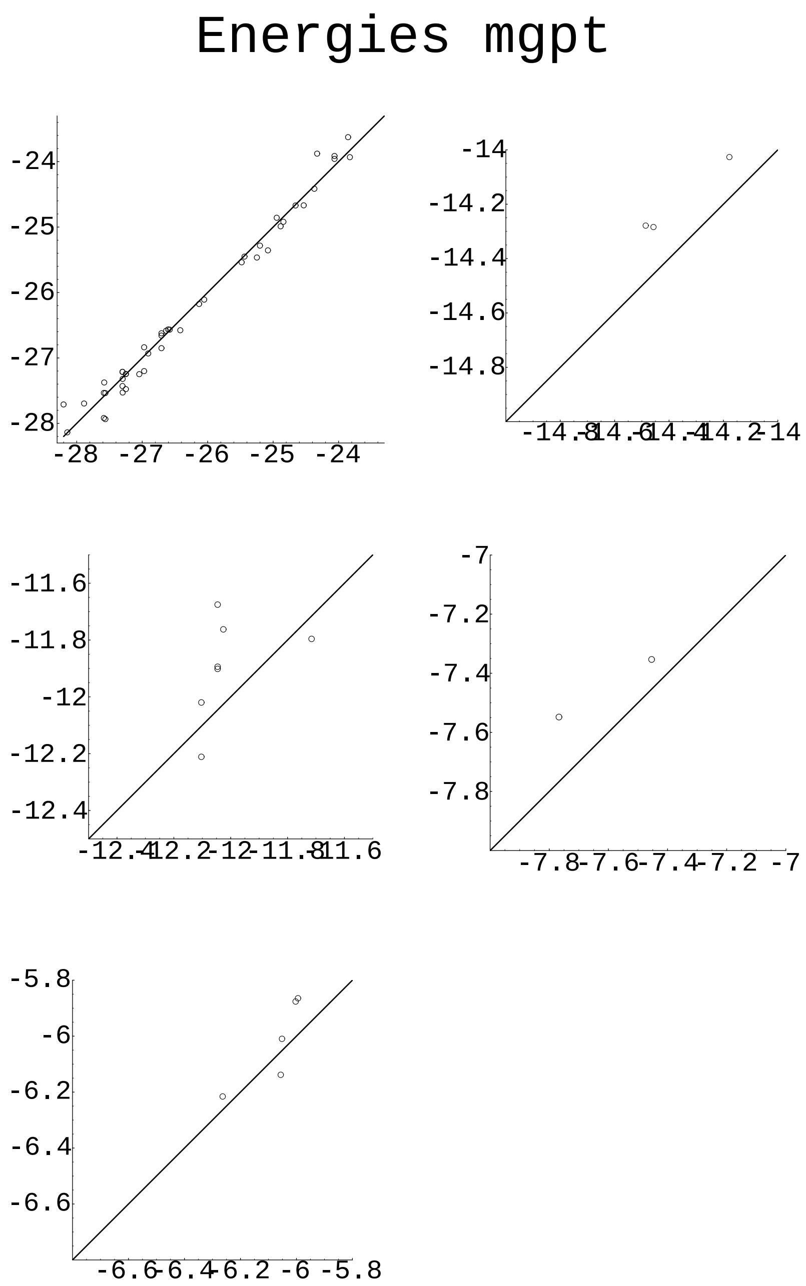

FIG. 10. Similar to figure 8 but for mGPT pair potential calculations